MUTATIONAL ANALYSIS OF THE VAM3 TRANSMEMBRANE DOMAIN AND ITS EFFECTS ON VACUOLE FUSION IN *SACCHAROMYCES CEREVISIAE*

BY

MING WU

THESIS

Submitted in partial fulfillment of the requirements
for the degree of Master of Science in Biochemistry
in the Graduate College of the
University of Illinois at Urbana-Champaign, 2013

Urbana, Illinois

Adviser:

Assistant Professor Rutilio Fratti

ABSTRACT

Vam3 is a SNARE protein essential in yeast vacuole homotypic fusion. The specific role of the Vam3 trans-membrane domain (TMD) during vacuole fusion remains unclear. Previous work had shown that replacing Vam3 TMD with a prenyl lipid anchor (CCIIM) results in attenuated fusion and accumulation of trans-SNARE complexes, indicating CCIIM can not transit enough energy to stimulate membrane fusion as Vam3 TMD does. Hypothesis were proposed that the either the length or the specific Vam3 TMD interactions with its cognate SNAREs, or a combination of both, result in the less efficient fusion with Vam3-CCIIM. In this study, I further studied the Vam3-CCIIM vacuole fusion and vacuole morphology. To test the above hypotheses, I constructed truncations at the C-terminus of the Vam3 TMD to study the effect of varying length of Vam3 TMD. To study the specific TMD interactions with other SNAREs, I mutated three non-aliphatic amino acids in the Vam3 TMD that may contribute to inter-helical interactions with cognate SNAREs. I also constructed the yeast mutant strains and found those mutations cause vacuole fragmentation. These mutants could be used for further studying their effect on fusion and protein complex formation, and deciphering Vam3 TMD's role during fusion.

Dedicated to my parents and my husband.

ACKNOWLEDGEMENTS

First and foremost, I thank my advisor, Dr. Rutilio "Rudy" A. Fratti, for his mentorship and support over the period of this research project. He shed light on the project by giving supportive criticism and wise suggestions. His positive feedback and overall optimism were always inspirational.

I would also like to thank Mark Padolina, Dr. Terry Sasser, Dr. Surya Karunakara, Nick DeSanto, Gus Lawrence, Colin Stoy, Mattew Starr, Gregory Miner, and all the undergraduates in the research group, who made the lab a friendly, supportive and productive environment.

Table of Contents

Chapter 1 Introduction

1.1 Yeast Vacuole Fusion

Membrane fusion is critical for maintaining cellular homeostasis, subcellular compartmnetalization, cell growth, hormone secretion and the release of neurotransmitters (1). The machinery for membrane fusion was found to be conserved from single-cellular eukaryotes, such as yeast, to evolutionarily more advanced mammals (2).

Yeast vacuole homotypic fusion is widely used as a model system for the study of membrane fusion because genetic manipulation in yeast is much easier than that in higher eukaryotes like mice. Moreover, yeast vacuoles are large organelles whose morphology can be well examined under a light microscope. Yeast vacuoles can also be readily harvested in large quantities, facilitating high-throughput experiments. Furthermore, a rapid and convenient in vitro colorimetric assay has been developed to measure the fusion of yeast vacuoles since purified vacuoles bear a full set of all the molecules necessary for fusion. Experiments that can reconstitute all-pure components in fusion are well established as well (1, 3).

Yeast vacuole fusion requires close cooperation of the following components: four SNARE proteins (soluble N-ethylmaleimide-sensitive factor attachment protein receptors), which include Nyv1, Vam3, Vti1, and Vam7, and their chaperones Sec18/NSF and Sec17/α-SNAP, a Rab family GTPase Ypt7, the hexameric tethering complex HOPS (homotypic fusion and protein sorting complex), composed of Vps11, Vps16, Vps18, Vps33, Vps39 and Vps41 as its 6 subunits, actins, and five regulatory lipids including ergosterol, phosphatidic acid, diacylglyerol, sphingolipids and phosphoinositides (4, 5, 6).

Vacuole fusion occurs on four steps: priming, tethering, docking and vertex assembly, hemifusion and fusion. During priming, cis-SNAREs (SNARE proteins on the same side of the

membrane) are disassembled by Sec18, releasing Sec17 (7), free SNAREs and soluable Vam7 (8). Next, the first molecular association between the two membranes that are about to fuse, termed 'tethering', is Ypt7 dependent (9, 10). Soluble Vam7 rebind to the membrane by the interaction between its PX domain and HOPS and phosphatidylinositol 3-phosphate (PI3P) on the membrane (9, 11). Next, SNARE proteins bind to each other forming SNARE complexes in trans (between two membranes) that triggers the releasing of luminal calcium (12, 13). The resulting tight association between docked vacuoles lead to the formation of two flattened discs of the two apposed membranes called boundary membranes. The perimeters of the boundary membranes are termed 'vertex ring' where proteins and regulatory lipids important in vacuole fusion are concentrated (14). With the completion of fusion, not only the lipid bilayers, but also the luminal content of the two vacuoles mix together.

First discovered in late 1980s, SNARE proteins are found crucial in membrane fusion, with their significance implicated by the fact that they are found in all organelles of exocytic and endocytic pathways, from yeast to man (15, 16). With several exceptions, most SNARE proteins are composed of a variable and independently-folded N-terminal domain, a coiled-coil SNARE motif and a C-terminal trans-membrane domain which functions as the membrane anchor. The SNARE motif is characteristic of SNARE proteins and is evolutionarily conserved (15). SNARE complexes formation is mediated by SNARE motifs, which can spontaneously associate into a four-helix bundle, with each helix provided by a different SNARE motif (17). The free energy released during SNARE complexes formation by SNAREs from opposite membranes leads to a tight connections between the opposing membranes and is thought to drive the membranes to fuse, resulting in trans-SNARE complexes converting to cis-SNARE complexes. The residues in the SNARE motifs are generally apolar, but the '0'-layer near the center of the 4-helix bundle are polar, composed of highly conserved 3 glutamine (Q) and 1 arginine (R) (18, 4). SNAREs are

then classified into Qa-SNAREs, Qb-SNAREs, Qc-SNAREs and R-SNAREs. Productive SNARE complexes requires the four-helix bundle formation by SNARE motifs from one of each of the Qa-, Qb-, Qc- and R-SNAREs (15). Vam3, Vti1 and Vam7 are the Qa-, Qb-, Qc-SNAREs and Nyv1 is the one R-SNARE in yeast homotypic vacuole fusion. Though most SNARE complexes have the QabcR combination, SNARE motifs can potentially associate in other combinations, such as Qaaaa complexes, Qabab complexes, Qaabc complexes. Thesse helical bundles with non-conventional combinations are less stable, and might not have the correct membrane topology, and are less capable of transit the energy to drive membrane fusion (15, 19, 20). Finally, after fulfilling their role in driving membrane fusion, SNARE complexes can be disassembled and recycled by Sec18/NSF and Sec17/α-SNAP in an ATP-dependent manner during the initial priming step of the next round of fusion.

1.2 Vam3

Vam3 is a 283-amino-acid-long protein. It has three N-terminal regulatory alpha helical domains (H_A, H_B and H_C, respectively), the SNARE motif, and the C-terminal helical trans-membrane domain (TMD).

Vam3 is essential for yeast homotypic vacuole fusion. Being a Qa-SNARE, Vam3 associates with Vam7, Vti1 and Nyv1 to form the four helix bundle with its SNARE motif to catalyze fusion.Vacuoles lacking Vam3 can not fuse normally (21, 22). Though the alpha-helical TMD of Vam3 was previously shown to be critical for productive priming and normal fusion (22), the specific mechanism of Vam3 trans-membrane domain during fusion remains unclear. Ungermann and colleagues made a Vam3-CCIIM chimera in which the trans-membrane domain of Vam3 protein was replaced by the prenylation motif from Ykt6. Vam3-CCIIM was localized to

vacuoles and expressed at levels comparable to wild-type Vam3 expression levels. However, fusion of Vam3-CCIIM was strongly attenuated, and had an increased amount of cis-SNARE complexes, indicating that Sec18-dependent priming and cis-SNARE complex disassenbly was attenuated. In fact, efficient cis-SNARE complex disassembly requires addition of exogenous Sec18. There is also an 4-fold increase in the amount of trans-SNARE complexes, indicating that Vam3-CCIIM cannot transit enough energy to stimulate membrane fusion and converting trans-SNARE complexes to cis-SNAREcomplexes. Furthermore, there is a 50% decrease in the palmitoylation of Vac8, which is required during early stages of priming (22).

The accumulation of trans-SNARE complexes containing Vam3-CCIIM indicates that the prenyl anchor CCIIM could not transit sufficient energy to the membranes to initiate fusion as the native Vam3 TMD can. Two hypothesis were proposed to explain it: first, lipid anchors only cross one leaflet of the membrane bilayer, so less energy could be transited through the lipid anchor than through the longer native Vam3 CCIIM. The alternative hypothesis is that the native Vam3 TMD has specific interactions with cognate SNAREs and changing it to a lipid anchor affects the formation of productive SNARE complexes, resulting in the inability for trans-SNARE complexes to trigger fusion. The second hypothesis is supported by several neuronal SNAREs studies. A structural study of the neuronal cis-SNARE complexes indicated that the alpha-helical bundle proceed beyond the SNARE motifs and continues into the linker region (a short region between the SNARE motif and the C-termianl TMD) and the TMD. It's noted that the continuous helical bundle is further stabilized by side-chain interactions in the linker region. It's unknown, however, whether the bundling of TMDs is important or whether there are any specific interactions between the TMDs of cognate vacuolar SNAREs (23). Another group found that truncated or deleted TMD of syntaxin have reduced binding affinities with synaptotagmin, α/β-SNAP, and synaptobrevin. Normal cognate protein binding could be

"rescued" by replacing the TMD of syntaxin with TMD of synaptobrevin and synaptotagmin. However, normal binding could not be rescued by fuse TMD-deleted syntaxin with TMD of other hydrophobic amino acids of the same length (1124). These findings strongly suggest the shorter length of CCIIM could not be the only reason for Vam3-CCIIM to fuse poorly, and it's most likely that both the length and specificity of SNARE TMD interactions contribute to efficient fusion.

Moreover, Vam3 trans-membrane domain can form homodimers via the TMD-TMD interactions (25). Replacing the native Vam3 TMD with a stretch of polyalanine disrupted the dimerization (25). Mutations that would disrupt dimerization of TMD of syntaxin won't impair the full-length syntaxin's binding with other cogante SNAREs, indicating a poor correlation between Vam3 TMD homodimerization and bundling of SNARE TMDs.

In order to further study the function of Vam3 trans-membrane during fusion and decipher the mechanism of attenuated fusion of Vam3-CCIIM, I constructed a series of mutants to test the two hypothesis as stated above. To test the first hypothesis, I truncated Vam3 TMD which can be used to test the effect of varying lengths of Vam3 TMD. To test the second hypothesis, I mutated several non-aliphatic amino acid sites in Vam3 TMD that could contribute to inter-helical interactions with other cognate SNAREs. These sites include an N-terminal T266, and C-terminal C274 and M275. I mutated each of these residues to alanine, and constructed a mutant containing all three mutations (Vam3-3Ala). I further constructed the mutant yeast strains, which can be used for studying their effect on fusion and protein complex formation.

Chapter 2 Materials and Methods

2.1 Strains

Yeast strains BJ Vam3-CCIIM (*MATα pep4::HIS3 prb1-Δ1.6R his3-200 lys2-801 trp1Δ101 (gal3) ura3-52 gal2 can1 Δ vam3Δ VAM3CCIIM::URA3*) and DKY Vam3-CCIIM (*MATα pho8::TRP1 leu2-3 leu 2-112 ura3-52 his3-Δ200 trp1-Δ901 lys2-801Δ vam3Δ VAM3CCIIM::URA3*) were used for the study of Vam3-CCIIM vacuole fusion and vacuole morphology. Yeast strains BJ3505 (*MATα pep4::HIS3 prb1-Δ1.6R his3-200 lys2-801 trp1Δ101 (gal3) ura3-52 gal2 can1*) and DKY6281 (*MATα pho8::TRP1 leu2-3 leu 2-112 ura3-52 his3-Δ200 trp1-Δ901 lys2-801*) were used as wild-type controls in vacuole fusion assay, microscopy analysis of vacuole fusion, colony PCR and Western blot.

CBP-Vam3 were cloned from yeast strain CBP-Vam3 (*MATa pho8::TRP1 leu2-3 leu 2-112 ura3-52 his3-Δ200 trp1-Δ901 lys2-801*). Mutant Vam3 plasmids were transformed into the following yeast strains: BJ ΔVam3 (*MATa pep4::HIS3 prb1-Δ1.6R his3-200 lys2-801 trp1Δ101 (gal3) ura3-52 gal2 can1 vam3Δ*) and DKY ΔVam3 (*MATa pho8::TRP1 leu2-3 leu 2-112 ura3-52 his3-Δ200 trp1-Δ901 lys2-801 vam3Δ*).

2.2 Vacuole Isolation and Fusion Assays

Yeast vacuoles were isolated by floatation with four-tiered ficoll gradient after the yeast cell wall were broken down by lyticase. Large amounts of vacuole could be isolated and purified in this way, and the amount of the vacuoles were quantified with a Bradford assay (26).

In vitro fusion reactions (30 μl) contained 3 μg with each of vacuoles from or derived from BJ3505 and DKY6281, fusion buffer (125 mM KCl, 5 mM $MgCl_2$, 20 mM PIPES-KOH pH 6.8, 200 mM Sorbitol), ATP regenerating system (1 mM ATP, 0.1 mg/ml creatine kinase, 29 mM

creatine phosphate), 10 μM coenzyme A, 283 nM inhibitor of protease B (IB_2). The reactions were incubated at 27°C for 1.5 hours, after which fusion was assayed by Pho8 activity in 250 mM Tris-HCL pH 8.5, 0.4% Triton X-100, 10 mM $MgCl_2$, 1 mM *p*-nitrophenylphosphate. One fusion units were measured as 1 μmol of *p*-nitrophenolate produced minute $^{-1}$, μg $^{-1}$ *pep4*Δ vacuoles. *p*-nitrophenolate absorbance was measured at 400 nm (27).

2.3 Molecular Cloning and Site-Directed Mutagenesis of CBP-Vam3

The CBP-Vam3 open reading frame was amplified from CBP-Vam3 yeast strains, using forward primer 5'-GCTGCGAAGCTTATGTCCTTTTTCGACATC-3' with a HindIII restriction site, and a reverse primer 5'-GCGGCCGGATCCCTAACTTAATACAGCAAG-3' with a BamHI restriction site. Digested PCR product was ligated to HindIII/BamHI-digested pRS416 to generate pRS416-CBP-Vam3p. The plasmid was transformed into *Escherichia coli* Turbo high efficiency competent cells (NEB) and grown on Luria broth with ampicillin. The plasmids re-isolated from the colonies was verified by dideoxynucleotide chain-termination sequencing.

With pRS416-CBP-*VAM3* being the template, a modified version of QuickChange mutagenesis were used to generate $Vam3^{T266A}$, $Vam3^{C274A}$, $Vam3^{M275A}$, $Vam3^{C274A/M275A}$, and $Vam3^{T266A/C274A/M275A}$. The primers for mutating these targeted sites contains a non-overlapping sequences at the primers 3' end as well as the conventional primer-primer overlapping sequences at the 5' end to minimize the primer dimer formation and enable the primers to use the newly-synthesized DNA as the template, thus promote the efficiency of site-directed mutagenesis (28). Since C274 and M275 are next to each other, I mutated both these sites during one round of mutagenesis using one pair of primers carrying both mutations. Primer used for mutating these sites are listed in Table 2. The primers were synthesized from Integrated DNA Technologies

(1710 Commercial Park, Coralville, Iowa 52241 USA). All the mutants were sequenced by ACGT, Inc. (35 Waltz Drive, Wheeling, IL 60090) and verified.

2.4 Construct of Vam3 Mutant Yeast Strains

To construct Vam3 mutant yeast strains, each of the mutant Vam3 plasmids, $Vam3^{T266A}$, $Vam3^{C274A}$, $Vam3^{M275A}$ and $Vam3^{T266A/C274A/M275A}$, were transformed into both BJ ΔVam3 and DKY ΔVam3 yeast strains, respectively, and grown on selective medium lacking uracil and containing ampicillin as the selection marker. Colonies grew after about 4 days, and no colonies grew for the negative control plates (BJ ΔVam3 and DKY ΔVam3 competent cells not transformed with mutant Vam3 plasmids). Yeast colony PCR and Western blot were used to verify the transformation.

2.5 Microscopy

Vacuole morphology was monitored as described (29). Incubate yeast cells with 5 μM FM4-64 fluorescent dye labeling yeast vacuolar membranes for one hour. Cells were then washed and continued grown for over 3 hours. Next, cells were washed with PBS buffer, concentrated, and mixed with poly-L-lysine and spread on glass slides for observation. Images were obtained with a Zeiss Axio Observer Z1 inverted fluorescent microscope equipped with an X-Cite 120XL light source, Plan Apochromat 63X oil objective and an AxioCam CCD camera. FM4-64 images were obtained with a 43 HE CY 3 shift-free filter set.

2.6 Vam3 Truncations

To generate a series of truncations of Vam3 in its C-terminal trans-membrane domain, the

Vam3 open reading frame, excluding last 3, 5, 7, 9 amino acid residues in the trans-membrane domain were amplified from DKY6281 yeast strains. The primers used were listed in Table 2. The forward primers carry a HindIII restriction site, and the reverse primers carry a EcoRI restriction site. Digested PCR products were then ligeated into double-digested pRS416 and transformed into *Escherichia coli* Turbo high efficiency competent cells (NEB) and grown on Luria broth with ampicillin. The plasmids re-isolated from the colonies was verified by dideoxynucleotide chain-termination sequencing.

Chapter 3 Results

3.1 Vam3-CCIIM

3.1.1 Vam3-CCIIM Vacuole Fusion Assay

Fusion was measured by the maturation of proPho8p (pro-alkaline phosphatase) by protease A (Pep4p) (29). These experiments used vacuoles from reciprocally deleted stranis DKY6281(*PEP4 pho8*Δ) and BJ3505 (*pep4*Δ *PHO8*). Previous study showed that Vam3-CCIIM fuses poorly, showing an 80% reduction in fusion relative to WT vacuoles (22). Previous work in our lab showed that fusion blocked by anti-Sec17 at the priming step can be bypassed by adding exogenous Vam7 as they can form SNARE complexes with free cognate SNAREs on the membrane and therefore fusion can go on (16). I used different combinations of vacuoles to repeat the Vam7 bypass fusion assays. One combination used WT and Vam3-CCIIM vacuoles at a 1:1 ratio, where the DKY6281 reporter strain contained WT Vam3 and the BJ3505 reporter strain harbored Vam3-CCIIM. Another combination used BJ3505 containing WT Vam3 and DKY6281 harbouring Vam3-CCIIM. A third combination used both reporter strains that harbored Vam3-CCIIM. For all of them, fusion could be inhibited by anti-Sec17, but could not be rescued by adding exogenous Vam7 alone. CPZ was used to see if fusion could be restored. CPZ is a small amphipathic molecule that can traverse the lipid bilayer and insert itself into the inner leaflet of membranes, and can therefore increase the negative curvature of the outer leaflet of the bilayer, believed to reduce the energy threshold for SNAREs-driven membrane fusion (30). For the first two combinations, where Vam3-CCIIM is only present on one side of the vacuoles and WT Vam3 is present on the other side of the vacuoles, fusion could be restored by adding CPZ. However, for the combinations where both strains harboured Vam3-CCIIM, CPZ is unable to restore fusion. Several Vam7 mutants, including Vam7^{Q283R}, Vam7^{Y42A}, Vam7 ΔCC, were able

to rescue fusion in the presence of CPZ, with WT DKY and Vam3-CCIIM BJ vacuoles, though to less extents (Figure 1).

3.1.2 Vam3-CCIIM Vacuole Morphology

Since Vam3-CCIIM affect yeast vacuole fusion, it's possible that Vam3-CCIIM would affect vacuole morphology. To examine the its vacuole morphology, DKY Vam3-CCIIM **y**east cells were incubated with 5 μM FM4-64 to label vacuoles. Cells were washed with PBS and grown for another 3 hours before mounted in poly-L-lysine for microscopy. Cells were photographed using DIC, and FM4-64 images were acquired using a 43 HE CY 3 shift-free filter set (29). DKY6281 (wild-type) were used as positive control and DKY Δ Vam3 were used as negative control. Previously, Vam3-CCIIM strains were shown to have a single large intact vacuole in each cell (22). However, I observed cells both harbouring large intact vacuoles, and small amounts of cells harbouring multiple or even fragmentted vacuoles in Vam3-CCIIM (Figure 2.1). After careful observation, quantification and statistical analysis of the number of vacuoles per cell in each cell type, it's observed that approximately 60% of Vam3-CCIIM cells harbouring a single vacuole per cell, while the rest of the cells may have 2, 3, 4, 5 or more fragemented vacuoles per cell. Most wild-type cells harhour a single intact vacuole per cell, while most of the Δ Vam3 cells have over 3 vacuoles per cell. So, Vam3-CCIIM's phenotype is an intermediate between that of wildtype and that of the deletion strain, indicating that Vam3-CCIIM is functional in vivo, though the functionality is impaired in comparison with the wild-type Vam3.

3.2 Vam3 TMD Mutations

3.2.1 Vam3 TMD Site-Directed Mutagenesis

First, CBP-Vam3 were cloned from CBP-Vam3 yeast strains as a template for mutagenesis. The calmodulin binding peptide (CBP) tag can facilitate future protein interaction study by CBP-pulldown assay. The CBP-Vam3 open reading frame was amplified from CBP-Vam3 yeast strain, using forward primer 5'-GCTGCGAAGCTTATGTCCTTTTTCGACATC-3' with a HindIII restriction site, and a reverse primer 5'-GCGGCCGGATCCCTAACTTAATACAGCAAG-3' with a BamHI restriction site (Table 2.). Digested PCR product was ligated to HindIII/BamHI-digested pRS416 to generate pRS416-CBP-Vam3p. The plasmid was transformed into *Escherichia coli* Turbo high efficiency competent cells (NEB) and grown on Luria broth with ampicillin. The plasmids re-isolated from the colonies was verified by dideoxynucleotide chain-termination sequencing.

With pRS416-CBP-*VAM3* being the template, I mutated T266, C274 and M275 to in the TMD of Vam3 to alanine. The three mutation sites were shown in Figure 3. A modified version of QuickChange mutagenesis protocol were used, which is more efficient than the conventional QuickChange protocol, with the success rate being approximately 25%. The primers for mutating these targeted sites contains a non-overlapping sequences at the primers' 3' end as well as the conventional primer-primer overlapping sequences at the 5' end to minimize the primer dimer formation and enable the primers to use the newly-synthesized DNA as the template, thus promote the efficiency of site-directed mutagenesis (28). Primer used for mutagenesis are listed in Table 2.

Creating the three single mutants ($Vam3^{T266A}$, $Vam3^{C274A}$, $Vam3^{M275A}$) were relatively quite easy, and were successful in the first two attempts. Since C274 and M275 are next to each other,

I then mutated both these sites during one round of mutagenesis using one pair of primers carrying both mutations. As mutating two sites at the same time causes more mismatches between the primers and the template, lower annealing temperature and less stringent conditions were used in the polymerase chain reaction (PCR). I also picked more colonies and sent more plasmids for sequencing. Vam3$^{C274A/M275A}$ were successfully created, though the mutagenesis success rate were slightly lower.

For creating Vam3$^{T266A/C274A/M275A}$ triple mutant, C274 and M275 were mutated on the pRS416-CBP-*VAM3*^{T266A} template. Several attempts were made before the triple mutant were obtained. Initially, the primer used were so long, though it carries C274A and M275A mutations, spans over T266 as well and unintentionally back mutate T266A to threonine. New primers were designed, with alanine at T266 site. Back mutations were avoided and Vam3$^{T266A/C274A/M275A}$ were made.

All the mutants, including Vam3^{T266A}, Vam3^{C274A}, Vam3^{M275A}, Vam3$^{C274A/M275A}$, and Vam3$^{T266A/C274A/M275A}$,as described above were verified by sequencing.

3.2.2 Vam3 Mutants Yeast Strains Construction

To construct Vam3 mutant yeast strains, each of the mutant Vam3 plasmids, Vam3^{T266A}, Vam3^{C274A}, Vam3^{M275A} and Vam3$^{T266A/C274A/M275A}$, were transformed into both BJ ΔVam3 and DKY ΔVam3 yeast strains, respectively, and grown on selective medium lacking uracil and containing ampicillin as the selection marker. After that, yeast genomic DNA were isolated from colonies of each of the new strains, and PCR using primers from upstrem and downstream of Vam3 open reading frame (CBP-Vam3-F and CBP-Vam3-R, as listed in Table 2) were performed to see if the transformation were successful. BJ3505 and DKY6281 were used as positive

controls and BJ ΔVam3 and DKY ΔVam3 were used as negative controls. The first several attempts were unsuccessful, as Vam3 DNA fragments were amplified not only from the transformed strains and positive controls, but also from BJ ΔVam3 and DKY ΔVam3. Different pairs of Vam3 primers were used in PCR with similar results. It's probable that the BJ ΔVam3 and DKY ΔVam3 yeast stock contained a mixture of wild-type and Vam3-deletion cells. So I spread BJ ΔVam3 and DKY ΔVam3 in uracil-dropout plates and picked single colonies, and use them as starting points for transformation.

After transformation, colonies grew after about 4 days, and no colonies grew for the negative control plates (BJ ΔVam3 and DKY ΔVam3 competent cells not transformed with mutant Vam3 plasmids). These colonies were verified by PCR. Yeast colony PCR, instead of isolating genomic DNA and using genomic DNA as the template to perform PCR, were used to accelerate the project. Vam3 could be amplified from BJ ΔVam3 and DKY ΔVam3 transformed with mutant Vam3 plasmids, and no Vam3 were amplified from BJ ΔVam3 and DKY ΔVam3 deletion strains (Figure 4). It's also noted that the size of Vam3 amplified from wild-type BJ3505 and DK6281 were slightly smaller than that from the deletion strains transformed with mutant Vam3 plasmids. It's consistent with the fact that mutant Vam3 plasmids carry a small CBP tag. The sequence coding CBP tag is about 50 bp. The yeast colony PCR results indicate that $Vam3^{T266A}$, $Vam3^{C274A}$, $Vam3^{M275A}$ and $Vam3^{T266A/C274A/M275A}$ were successfully transformed into BJ ΔVam3 and DKY ΔVam3 yeast strains, and Vam3 mutant yeast strains were created.

3.2.3 Vam3 Mutants Vacuole Morphology

The same method for observing Vam3-CCIIM vacuole morphology were used to observe DKY $Vam3^{T266A}$, $Vam3^{C274A}$, $Vam3^{M275A}$, and $Vam3^{T266A/C274A/M275A}$ vacuole morphology. DKY

ΔVam3 were used as negative controls, and the DKY6281 were used as positive controls. Each type of Vam3 mutant cells contained fragmented and deformed vacuoles (Figure 5.1). A statistical analysis were made to quantify the number of vacuoles per cell for each cell type(Figure 5.2). Almost all wild-type cells contain a single vacuole per cell, and ΔVam3 cells are highly fragmented cells. Over 90% of DKY $Vam3^{T266A}$, $Vam3^{C274A}$, $Vam3^{M275A}$, and $Vam3^{T266A/C274A/M275A}$ cells were fragmented, but they have a higher proportion of cells containing one of two vacuole per cell than ΔVam3 cells. It's also noted that most yeast vacuoles has a diameter of 5-6.5 μm, while in BJ $Vam3^{3Ala}$ extraordinarily large vacuole with a diameter of 9-10 μm were observed (Figure 5.3).

3.3 Vam3 TMD Truncations

In order to study the effect of varying lenght in Vam3 TMD, a couple of truncations in the C-terminal of the TMD were made.The plasmids were made by amplifying the Vam3 open reading frame, excluding last 5, or 9 amino acid residues in the trans-membrane domain from DKY6281 yeast strains. The primers used were listed in Table 2. The forward primers carry a HindIII restriction site, and the reverse primers carry a EcoRI restriction site. Digested PCR products were then ligeated into double-digested pRS416 and transformed into Escherichia coli Turbo high efficiency competent cells (NEB) and grown on Luria broth with ampicillin. The plasmids re-isolated from the colonies was verified by dideoxynucleotide chain-termination sequencing.

Chapter 4 Discussion

4.1 Vam3-CCIIM

Vam3-CCIIM vacuoles fuse poorly compared to the wild-type, indicating the importance of Vam3 trans-membrane domain in yeast vacuole fusion. For wild-type Vam3, blocked the priming stage with anti-Sec17 could be bypassed by adding exogenous Vam7p. However, Vam3-CCIIM on one side or both sides of the vacuoles cannot promote fusion in Vam7 bypass fusion assays. By adding CPZ, fusion could be restored when Vam3-CCIIM is present on one side of the vacuoles, but fusion could not be restored when both sides of the fusion pairs carry Vam3-CCIIM. It suggest that wild-type Vam3 on one side of the vacuole is capable of transit sufficient energy to drive fusion, with the help of CPZ. When Vam3 is absent on both sides of vacuoles, Vam3-CCIIM cannot generate and transit sufficient energy for fusion.

Most Vam3-CCIIM cells harbouring a single vacuole, but there is a sharp increase in cells harbouring multiple vacuoles. It suggests that Vam3-CCIIM is able to function in vivo, but this functionality is somewhat impaired.

4.2 Vam3 TMD Mutations

In order to study the specific interactions between the Vam3 TMD with the TMDs of cognate SNAREs, a mutational study was made. Three non-aliphatic amino acids in the Vam3 TMD that could contribute to inter-helical interactions with other cognate SNAREs were mutated to alanine. These sites include an N-terminal T266, and C-terminal C274 and M275. Using pRS416-CBP-*VAM3* as the template, Vam3 TMD mutations including Vam3^{T266A}, Vam3^{C274A}, Vam3^{M275A} a, Vam3$^{C274A/M275}$ and Vam3$^{T266A/C274A/M275A}$ were constructed. The corresponding mutant yeast strains were obtained by transformation and verified by colony PCR. These mutants

causes vacuole fragmentation, indicating impaired functionality in vivo. BJ Vam3$^{T266A/C274A/M275A}$, in particular, showed sporadic extraordinarily large vacuoles. The abnormally large vacuoles may result from changed homeostasis and membrane fusion. Though the possibility that they're due to altered physiological status of that specific strain could not be excluded at present. All the mutants, especially Vam3$^{T266A/C274A/M275A}$ could be used in experiments like CBP-pulldowns, vacuole fusion assays, etc, to determine their effect on protein complex formation and fusion, and shed light on the specificity of Vam3 TMD interactions. The pRS416-CBP-*VAM3* I constructed could be used as a template to generate other Vam3 mutations if needed. Moreover, there is little mutational analysis in the transmembrane domain of other SNAREs. Two polar residues at S197 and Y198 in the TMD of Vti1, and S244 in the TMD of Nyv1 may be critical in the interaction between SNARE TMDs. The same method of constructing Vam3 mutants is applicable to create Vti1^{S197A}, Vti^{Y198A} and Nyv1^{S244A}.

4.3 Vam3 TMD Truncations

To examine the effect of varying lengths of the Vam3 TMD, a couple of Vam3 TMD truncations were created. In the future, corresponding yeast strains will be generated and their effect on SNARE complex formation, priming and fusion will be examined. If fusion is significantly reduced in Vam3 TMD truncations, the length of the Vam3 TMD is a major factor for its function in fusion, and the impaired fusion in Vam3-CCIIM should be at least partially attributed to the shorter length of the lipid anchor. If fusion is unaltered in Vam3 TMD, the second hypothesis is more likely to be correct.

Tables and Figures

Table 1. Yeast strains used in this study

Strain	Genotype	Source
BJ3505	*MATα pep4::HIS3 prb1-Δ1.6R his3-200 lys2-801 trp1Δ101 (gal3) ura3-52 gal2 can1*	Jones
DKY6281	*MATα pho8::TRP1 leu2-3 leu 2-112 ura3-52 his3-Δ200 trp1-Δ901 lys2-801*	Klionsky
BJ Vam3-CCIIM	BJ3505, *vam3Δ VAM3CCIIM::URA3*	Ungermann
DKY Vam3-CCIIM	DKY6281, *vam3Δ VAM3CCIIM::URA3*	Ungermann
CBP-Vam3	DKY6281, *vam3Δ CBP-VAM3::URA3*	Wickner
BJ ΔVam3	BJ3505 *vam3Δ*	Wickner
DKY ΔVam3	DKY6281 *vam3Δ*	Wickner
BJ Vam3^{T266A}	BJ3505, vam3Δ *VAM3^{T266A}::URA3*	This Study
BJ Vam3^{C274A}	BJ3505, *vam3Δ VAM3^{C274A}::URA3*	This Study
BJ Vam3^{M275A}	BJ3505, *vam3Δ VAM3^{M275A}::URA3*	This Study
BJ Vam3^{3A}	BJ3505, *vam3Δ VAM3$^{T266A/C274A/M275A}$::URA3*	This Study
DKY Vam3^{T266A}	DKY6281, *vam3Δ VAM3^{T266A}::URA3*	This Study
DKY Vam3^{C274A}	DKY6281, *vam3Δ VAM3^{C274A}::URA3*	This Study
DKY Vam3^{M275A}	DKY6281, *vam3Δ VAM3^{M275A}::URA3*	This Study
DKY Vam3^{3A}	DKY6281, *vam3Δ VAM3$^{T266A/C274A/M275A}$::URA3*	This Study

Table 2. Primers used in this study

Purpose	Primers	Sequences
Cloning CBP-Vam3	CBP-Vam3-F	5'-GCTGCGAAGCTTATGTCCTTTTTCGACATC-3'
	CBP-Vam3-R	5'-GCGGCCGGATCCCTA ACTTAATACAGCAAG-3'
Mutagenesis	Vam3^{T266A}-F	5'-GGTCGCCCTAATCATTATAATAGTTGTGTGCATGGTGGTATTG-3'
	Vam3^{T266A}-R	5'-TTATAATGATTAGGGCGACCTTACCGCATTTGTTACGGTC-3'
	Vam3^{C274A}-F	5'-AGTTGTGGCCATGGTGGTATTGCTTGCTGTATTAAGTTA G-3'
	Vam3^{C274A}-R	5'-ACCATGGCCACAACTATTATAATGATTAGGGTGACCTTACCG-3'
	Vam3^{M275A}-F	5'-AGTTGTGTGCGCGGTGGTATTGCTTGCTGTATTAAGTTAG-3'
	Vam3^{M275A}-R	5'-CCGCGCACACAACTATTATAATGATTAGGGTGACCTTACCG-3'
	Vam3$^{C274A/M275A}$-F	5'-AGTTGTGGCCGCGGTGGTATTGCTTGCTGTATTAAGTTAG-3'
	Vam3$^{C274A/M275A}$-R	5'-ACCGCGGCCACAACTATTATAATGATTAGGGTGACCTTACCG-3'
Truncations	Vam3-F	5'-GCTGCGAAGCTTATGTCCTTTTTCGACATC-3'
	Vam3-T2-R	5'-GCGGTCGAATTCCAATACCACCATGCACAC-3'
	Vam3-T4-R	5'-GCGGCCGAATTCGCACACAACTATTATAATG-3'

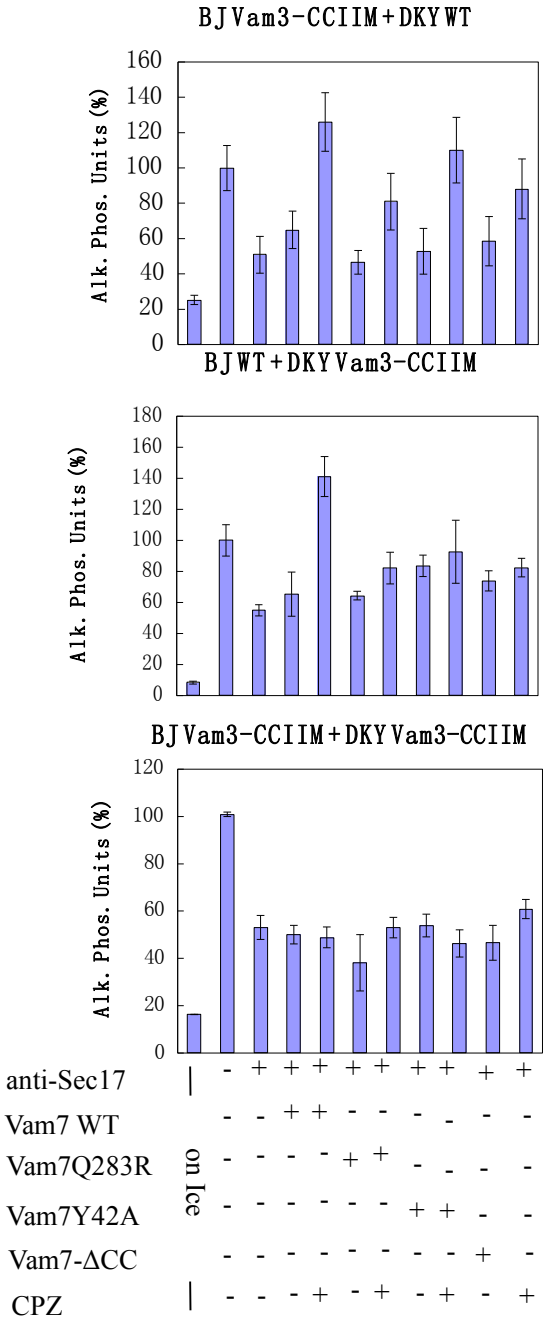

Figure 1. Vam3-CCIIM fusion assay. Three combinations of vacuoles were used for the fusion assay. The first combination used Vam3-CCIIM on BJ vacuoles and WT Vam3 on DKY vacuoles. The second used WT Vam3 on BJ vacuoles and Vam3-CCIIM on DKY vacuoles. The third combination used Vam3-CCIIM on both BJ and DKY vacuoles. Reactions were treated with buffer or anti-Sec17 to block priming. Bypassing the priming block was attempted with Vam7, $Vam7^{Q283R}$ (Q283R), $Vam7^{Y42A}$(Y42A), Vam7-ΔCC (ΔCC) in the presence or absence of chlorpromazine (CPZ). A reaction treated on ice were the negative control.

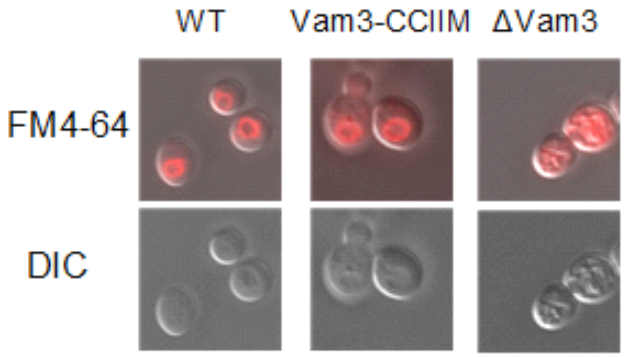

Figure 2.1. Vam3-CCIIM vacuole morphology. DKY Vam3-CCIIM Yeast cells were incubated with 5 μM FM4-64 to label vacuoles. Cells were washed with PBS grown for another 3 hours before mounted in poly-L-lysine for microscopy. Cells were photographed using DIC, and FM4-64 images were acquired using a 43 HE CY 3 shift-free filter set. DKY6281 (wild-type) were used as the positive control and DKY ∆ Vam3 were used as the negative control.

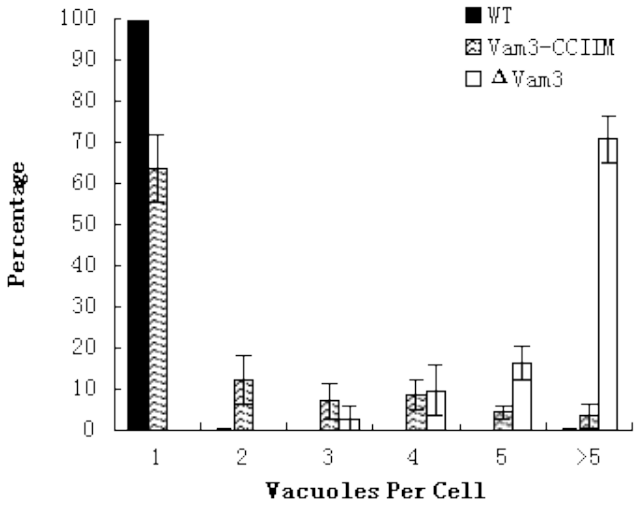

Figure 2.2. Quantification of the number of vacuoles per cell in Vam3-CCIIM. Vacuole morphology of DKY6281 (wild-type), DKY Vam3-CCIIM and DKY Δ Vam3 were studied under fluorescence microscope, and the number of vacuoles per cell in each cell type were quantified. For each cell type, over 100 cells were counted, and the experiment was repeated for 3 times.

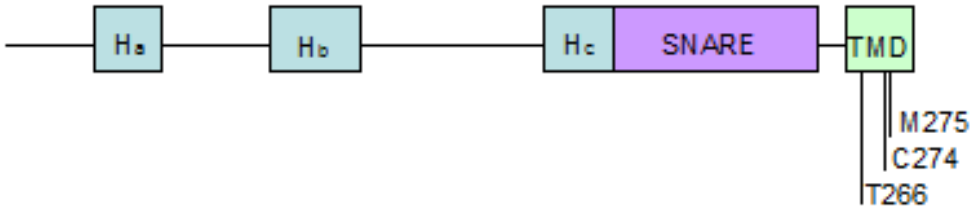

Figure 3. Vam3 mutation sites. Vam3p has three N-terminal alpha helical domains (H_A, H_B and H_C, respectively), a SNARE motif, and the C-terminal trans-membrane domain (TMD). Three non-aliphatic amino acid sites in Vam3 TMD, that could contribute to inter-helical interactions with other cognate SNAREs were mutated to alanine in this study. These three sites, including an N-terminal T266, and C-terminal C274 and M275, were shown in the graph.

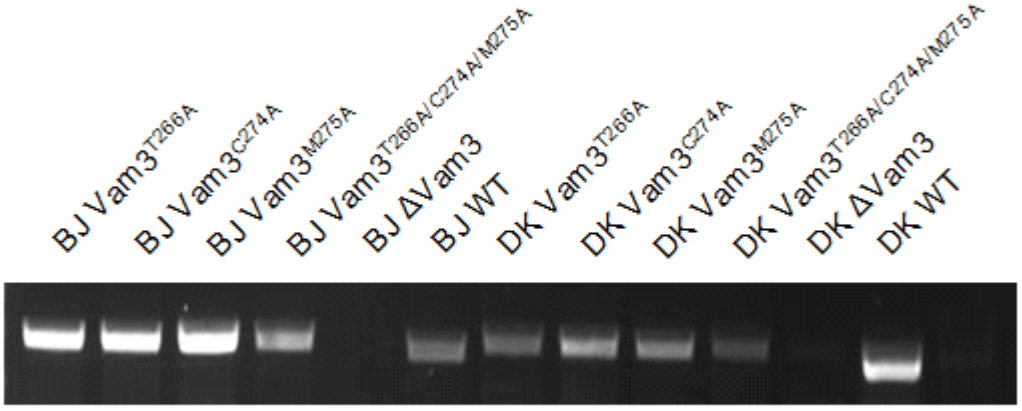

Figure 4. Verification of Vam3 mutant yeast strains by PCR. $Vam3^{T266A}$, $Vam3^{C274A}$, $Vam3^{M275A}$ and $Vam3^{T266A/C274A/M275A}$ were transformed into BJ ΔVam3 and DKY ΔVam3 yeast strains. Yeast colony PCR were performed to verify Vam3 mutant yeast strains. BJ3505 and DKY6281 were used as positive controls and BJ ΔVam3 and DKY ΔVam3 were used as negative controls.

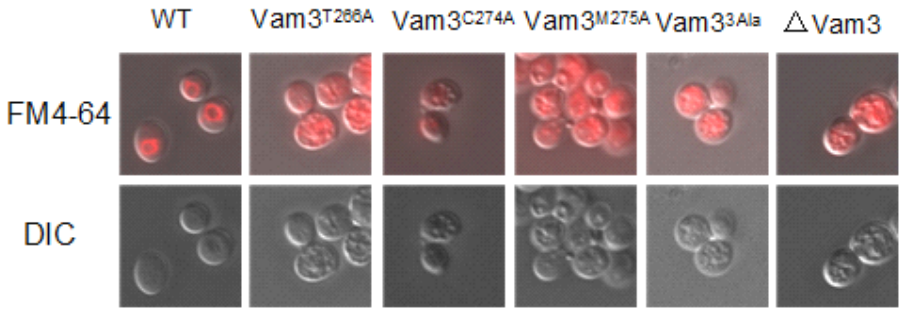

Figure 5.1. Mutation in Vam3 causes vacuole fragmentation. Mutant Vam3p vacuole morphology. Vam3 mutant cells were incubated with 5 μM FM4-64 to label vacuoles. Cells were washed with PBS grown for another 3 hours before mounted in poly-L-lysine for microscopy. Cells were photographed using DIC, and FM4-64 images were acquired using a 43 HE CY 3 shift-free filter set. DKY6281 (wild-type) were used as the positive control and DKY Δ Vam3 were used as the negative control.

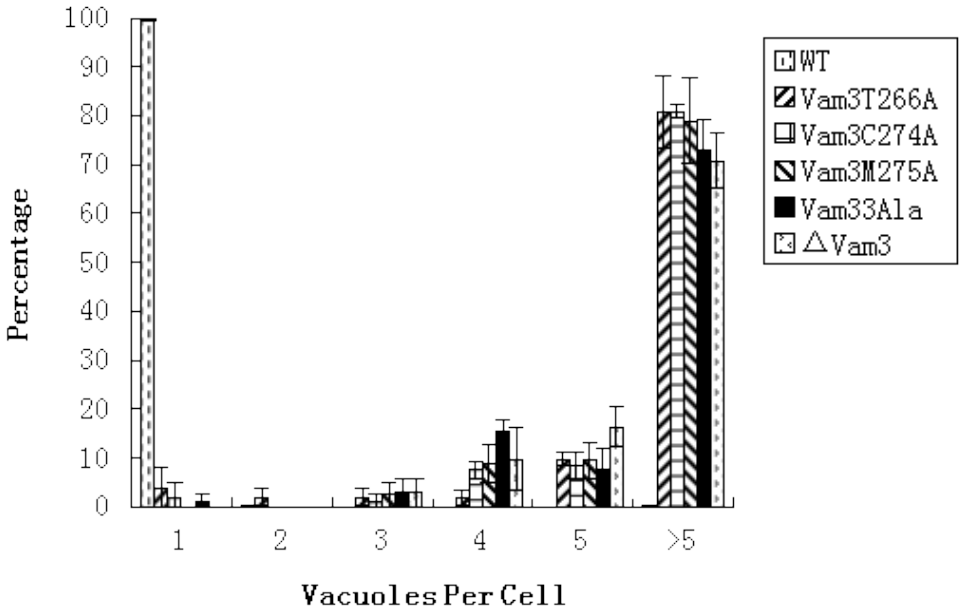

Figure 5.2. Quantification of the number of vacuoles per cell in mutant Vam3. Vacuole morphology of DKY6281 (wild-type), DKY $Vam3^{T266A}$, $Vam3^{C274A}$, $Vam3^{M275A}$, $Vam3^{3Ala}$ and DKY ∆ Vam3 were studied under fluorescence microscope, and the number of vacuoles per cell in each cell type were quantified. For each cell type, over 100 cells were counted, and the experiment was repeated for 3 times.

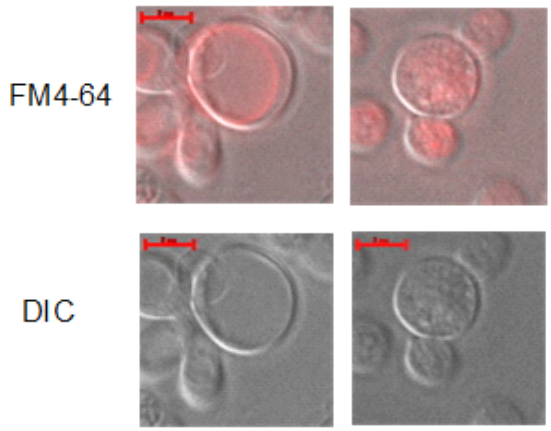

Figure 5.3. Occasional abnormally large vacuole of BJ Vam3^{3Ala}. Most yeast vacuoles has a diameter of 5-6.5 μm, while occasionally extraordinarily large vacuole with a diameter of 9-10 μm were observed in BJ Vam3^{3Ala}.

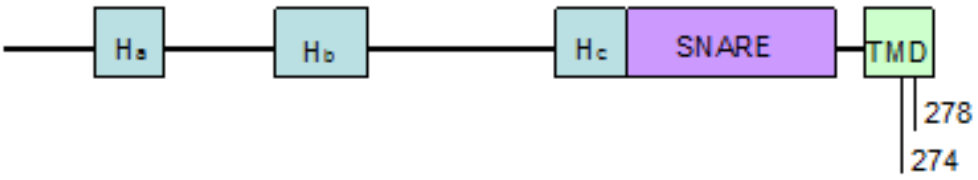

Figure 6. Vam3 mutation sites. Truncations of Vam3 TMD were generated to study the effect of varying length of Vam3 TMD. The truncation sites were shown in the graph.

References

1. Wickner, W., and Schekman, R. (2008) Nat Struct Mol Biol 15, 658-664
2. Jahn, R., and Sudhof, TC. (1999). Annu Rev Biochem 68:863-911
3. Wickner, W. (2010) Annu. Rev. Cell Dev. Biol 26:10.1-10.22
4. Fratti, R. , Y. Jun, A. J. Merz, N. Margolis, and W. Wickner. (2004) J Cell Biol 167:1087-98
5. Fasshauer, D., W. K. Eliason, A. T. Brunger, and R. Jahn. (1998) Biochemistry 37:10354-62
6. Jun, Y., R. A. Fratti, and W. Wickner. (2004) J Biol Chem 279:53186-53195
7. Mayer, A., W. Wickner, and A. Haas. (1996) Cell 85:83-94
8. Boeddinghaus, C., A. J. Merz, R. Laage, and C. Ungermann. (2002) J Cell Biol 157:79-89
9. Haas, A., D. Scheglmann, T. Lazar, D. Gallwitz, and W. Wickner. (1995) Embo J 14:5258-70
10. Mayer, A., and W. Wickner. (1997) J Cell Biol 136:307-17
11. Stroupe, C., K. M. Collins, R. A. Fratti, and W. Wickner. (2006) Embo J 25:1579-89
12. Ungermann, C., K. Sato, and W. Wickner. (1998) Nature 396:543-8
13. Merz, A. J., and W. Wickner. (2004) J Cell Biol 164:195-206
14. Wang, L., A. J. Merz, K. M. Collins, and W. Wickner. (2003) J Cell Biol 160:365-74
15. Jahn, R., and Scheller, R. H. (2006) Nat Rev Mol Cell Biol 7, 631-643
16. Fratti, R. A., Collins, K. M., Hickey, C. M., and Wickner, W. (2007) J Biol Chem 282, 14861-14867
17. Sutton, R. B., Fasshauer,D., Jahn, R., and Brunger,A.T. (1998)Nature 395, 347–353
18. Fasshauer, D., Eliason,W. K., Brunger, A. T., and Jahn, R. (1998) Biochemistry 37, 10354–10362
19. Fasshauer, D. (2003) Biochim. Biophys. Acta 1641, 87–97
20. Fasshauer, D. (2003) Biochim. Biophys. Acta 1641, 87–97
21. Wada Y., Nakamura N., Ohsumi Y., Hirata A. (1997) J. Cell Sci. 110:1299-1306
22. Rohde, J., Dietrich, L., Langosch, D., and Ungermann, C. (2003) J Biol Chem 278, 1656-1662
23. Stein, A., G. Weber, M. C. Wahl, and R. Jahn. (2009) Nature 460:525-8.
24. Lewis, J. L., M. Dong, C. A. Earles, and E. R. Chapman. (2001) J Biol Chem 276:15458-65.
25. Roy, R., K. Peplowska, J. Rohde, C. Ungermann, and D. Langosch. (2006) Biochemistry 45:7654-60.
26. Haas, A. (1995) Methods in Cell Science 17, 283-294
27. Haas, A., Scheglmann, D., Lazar, T., Gallwitz, D., and Wickner, W. (1995) Embo J 14, 5258-5270
28. Liu, H., and Naismith, J. H. (2008) BMC Biotechnol 8, 91

29. Quan-Sheng, Q., and Fratti, R. A. (2010) J Cell Sci 123, 3266-3275
30. Oghalai, J. S., H. B. Zhao, J. W. Kutz, and W. E. Brownell. (2000) Science 287:658-61